PAPER

Impedance spectroscopy applied to the fast wounding dynamics of an electrical wound-healing assay in mammalian cells

To cite this article: Mariela I Bellotti *et al* 2015 *Meas. Sci. Technol.* **26** 085701

IOP Publishing Measurement Science and Technology
Meas. Sci. Technol. **26** (2015) 085701 (11pp) doi:10.1088/0957-0233/26/8/085701

Impedance spectroscopy applied to the fast wounding dynamics of an electrical wound-healing assay in mammalian cells

Mariela I Bellotti, Fabián E Giana and Fabián J Bonetto

Laboratorio de Cavitación y Biotecnología, Instituto Balseiro/CAB-CONICET, 8400 San Carlos de Bariloche, Río Negro, Argentina

E-mail: fabian.giana@ib.edu.ar

Received 15 July 2014, revised 26 March 2015
Accepted for publication 15 April 2015
Published 25 June 2015

Abstract

Electrical wound-healing assays are often used as a means to study *in vitro* cell migration and proliferation. In such analysis, a cell monolayer that sits on a small electrode is electrically wounded and its spectral impedance is then continuously measured in order to monitor the healing process. The relatively slow dynamics of the cell healing have been extensively studied, while those of the much faster wounding phase have not yet been investigated. An analysis of the electrical properties of a particular cell type during this phase could give extra information about the changes in the cell membrane due to the application of the wounding current, and could also be useful to optimize the wounding regime for different cell types. The main issue when trying to register information about these dynamics is that the traditional measurement scheme employed in typical wound-healing assays doesn't allow the simultaneous application of the wounding signal and measurement of the system's impedance. In this paper, we overcome this limitation by implementing a measurement strategy consisting of cycles of fast alternating low- and high-voltage signals applied on electrodes covered with mammalian cells. This approach is capable of registering the fast impedance changes during the transient regime corresponding to the cell wounding process. Furthermore, these quasi-simultaneous high- and low-voltage measurements can be compared in order to obtain an empirical correlation between both quantities.

Keywords: wound-healing, cell wounding dynamics, mammalian cells, impedance spectroscopy, nonlinear voltage–current relationship

(Some figures may appear in colour only in the online journal)

1. Introduction

When cultured under standard conditions, a cell monolayer can be deliberately damaged to perform a so-called wound-healing assay. Traditionally, a mechanical, *in vitro* wound-healing assay is carried out by physically removing (e.g. with the tip of a micropipette) a portion of a cell monolayer, in order to obtain a cell-free region over the culture substrate. The damaged surface, which no longer contains cells attached to it, is therefore available for the surrounding, non-damaged cells, which tend to grow and migrate until completely re-covering this area. This kind of assay provides information about cell migration and proliferation, which take place in many biological processes, both physiological and pathological. Numerous similar assays have been used to study collective cell migration in a variety of biological processes, such as tissue repair, embryogenesis and cancer metastasis [1].

One of the major limitations of a mechanical wound-healing assay is the difficulty to define the exact area of the damaged surface, which is important for the quantification and reproducibility of the results. This limitation was overcome by the development, among others, of an electrical

wound-healing assay [2] based on the Electric Cell-substrate Impedance Sensing (ECIS™) technique [3]. ECIS is a recognized method for studying *in vitro* cell behaviour, based on the non-invasive, real-time monitoring of a cell culture's electrical properties. In addition to its application on wound-healing assays, ECIS was extensively employed to study cell spreading and attachment [4], differentiation [5], citotoxicity [6], differences between normal and transformed cells [7, 8], pathologies evaluation [9], etc.

In an ECIS-based wound-healing assay, a cell monolayer that sits on a gold microelectrode is first wounded by circulating a relatively high electrical current, and the time evolution of its electrical properties is afterwards registered. This data gives information about the cell migration and proliferation to re-populate the damaged surface, i.e. the healing process. In contrast with the mechanical wound-healing assay, by this method it is possible to exactly determine the area of the wound and also to control the intensity of the wounding signal.

Many studies were performed in order to characterize the wound healing behaviour of different cell types [10–13], and even an impedance imaging system was developed and used to monitor cell migration after wounding a cell monolayer [14]. However, to our knowledge still no emphasis was placed on the cell behaviour during the fast transient part of the assay, i.e. while the wounding current is being applied. The way in which cells are altered due to the application of high currents could give extra information about their morphological and structural characteristics, particularly about the changes in the cell membrane and in the cell adhesion. This information, together with the corresponding healing curves, could lead to a better understanding of a particular cell type's wound-healing behaviour. The purpose of this work is to introduce a measurement technique capable of registering information about the previously mentioned dynamics.

By means of an electrical wound-healing assay performed with a typical ECIS measurement scheme, it can be shown that the effects of the cell wounding take place entirely while circulating the electrical current, after which the wound starts to heal and no further damage is registered [2]. This implies that, in order to obtain information about the dynamics of the wounding phase of the assay, it is necessary to measure the system's impedance while applying the relatively high wounding electrical current. Also, due to the fast nature of the physical changes involved in this phase, it is mandatory to reach a high measurement speed in order to register these changes. These conditions motivated the implementation of an alternative measurement scheme, based on a computer-controlled LCR-meter capable of measuring impedance values at high speed, multiple frequencies and voltages up to $2\,V_{RMS}$. We first analysed the electrical response of Madine–Darby Canine Kidney (MDCK) cells at different measurement voltages, in order to determine the minimum voltage capable of inducing cell wounding with this measurement setup. Two different measurement strategies were then employed to register the fast impedance changes during the wounding phase of the assay. Details on these strategies will be given in section 2.3. The results are satisfactory, and this measurement technique can be used to obtain time-dependent spectral responses of cell-covered microelectrodes during the process of cell wounding.

2. Materials and methods

2.1. Cell culture

A Madin–Darby Canine Kidney (MDCK) [15] cell line was obtained from Banco Argentino de Células (Argentine Cells Bank, BAC). We selected this cell line because it represents a general model for epithelial cells, it was used in many studies involving impedance spectroscopy [2, 16–18] and its electrical response is well-known, therefore serving as a reference to which we can compare our results. For the experiments presented in this work, we used two cell suspensions with passage numbers 62 and 69. They were cultured under standard conditions (37 °C, 5% CO_2). Dulbecco's modified Eagle's medium (DMEM F-12, Gibco) was used as the culture medium, and was supplemented with 10% bovine fetal serum, 1% antibiotic-antifungus solution (penicillin, streptomycin, fungizone) and 2% HEPES buffer [19]. The measured conductivity of the medium was 19, 22 $mS\,cm^{-1}$.

The culture medium was changed approximately three times a week, and cell suspensions were prepared using standard trypsinization procedures (0.05% w/v trypsin—0.53 mM EDTA·4Na). Suspensions were made both for subcultivation purposes and for measurement of electrical properties. Cells were passaged at approximately 70% confluence, which was controlled by microscope examination.

The electrodes were incubated with media for approximately 20 h before seeding the cells. Proteins existing in the media pretreated the electrode surface, enhancing the attachment of cells. Cells were harvested from a 25 cm^2 flask (Nalgene) and plated at a density of 10^5 cells ml^{-1} in ECIS wells.

2.2. Measurement setup

The ECIS technique basically consists of measuring the impedance spectrum of a cell monolayer that sits on top of a small circular microelectrode made of gold [3]. A large counter-electrode (electrical ground) is the other electrical contact. The culture medium acts as an electrolyte and closes the electrical circuit. In this work we used microelectrodes measuring 250 μm in diameter of an ECIS Cultureware™ multiwell from Applied BioPhysics, which has an opaque outer surface.

The experiments presented in this work were carried out with a measurement setup consisting of a LCR-meter (Agilent Technologies, E4980a, California, USA) and a personal computer that both controls the experiment and stores the resulting data. The system was configured for a Kelvin sensing with 4-terminals (figure 1). Impedance measurements were performed by applying a voltage sine of $20\,mV_{RMS}$ directly on the electrode, producing an ac current of less than $1\,\mu A_{RMS}$, which is harmless for the cells [2]. The LCR-meter was connected to a personal computer through an USB interface and controlled with custom-made software, and its measurement function was set to a series-equivalent *RC* circuit (C_S–R_S). The

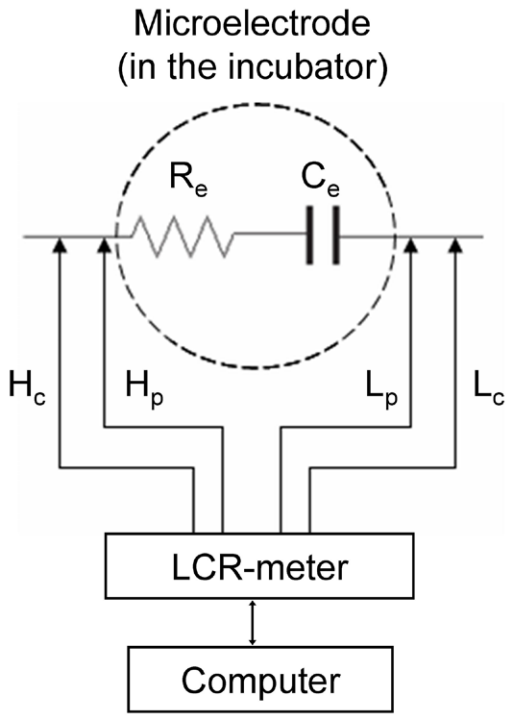

Figure 1. Schematic of the four-terminal, LCR-meter-based measurement setup (Kelvin method). The dotted circle represents the cell-covered microelectrode, modelled as a series RC circuit. R_e: equivalent resistance. C_e: equivalent capacitance. H_c: high-current terminal. H_p: high-potential terminal. L_c: low-current terminal. L_p: low-potential terminal.

measurements were carried out continuously at 10 different and logarithmically separated frequencies from 415 Hz to 50 kHz, in order to obtain the time-dependent impedance spectra.

Figure 1 shows the four-terminal connection between the LCR-meter and the ECIS microelectrode. The signal current path is defined by the high- and low-current terminals (H_c and L_c), while the voltage drop through the microelectrode is measured between the high- and low-potential terminals (H_p and L_p). This configuration has the advantage of minimizing the errors caused by the lead impedances and contact resistances [20]. The connection between the LCR-meter and the ECIS electrodes was outside the incubator.

Due to the fast dynamics of the process under study, the LCR-meter was configured to measure at its maximum speed by setting its measurement time to 'short', obtaining a single-frequency measurement approximately every tenth of a second or, equivalently, one spectrum per second. Although this measurement mode is the least accurate, it was sufficient to obtain representative values, as will be shown later.

2.3. Measurement strategies

The wound-healing assay was performed once the measured electrical properties reached a stationary state. The LCR-meter was then configured to produce a wounding signal which consisted on a sinusoidal wave in the range of 1.2–2 V_{RMS} at 50 kHz with a short measurement time. This specific frequency was selected to ensure high and uniform electric fields [2], and the wounding voltage range was chosen after analysing the electrical response of the cells at different voltages (section 3.2). Impedance data was registered during the whole process, including the fast wounding phase, and the experiments were repeated in different wells containing cells. In order to obtain this data, two different measurement strategies were employed, constituting an approach which is different from the established commercial wound-healing assays.

The first strategy was to apply the wounding signal continuously for 30 s and use it to measure the system's impedance. Although this method made it possible to obtain high-resolution, time-resolved curves of the resistance and capacitance changes during the wounding phase, its principal disadvantage was that the measurements were taken at a fixed frequency of 50 kHz, whereas a spectral response would prove a better set of data in order to achieve a precise biological interpretation of the results. Another issue with this measurement technique was a discontinuity observed in the resistance and capacitance curves due to the different measurement voltages, namely 20 mV_{RMS} before and after the wounding phase, and 1.2–2 V_{RMS} during this phase. This will be discussed in more detail in section 3.2.

The second measurement strategy consisted of alternating one second of the wounding signal with a fast ten-frequency measurement at 20 mV_{RMS}, repeating this procedure until the total application time of the wounding signal was 10 min. This higher exposure time was set with the purpose of ensuring the registration of the whole dynamics of the cell wounding, i.e. between the stationary states corresponding to the cell-covered electrode and the so-called naked electrode (with culture medium and devoid of cells). Figure 2 shows the RMS voltage and the frequency of the generated sinusoidal signal as a function of time for a wounding voltage of 1.2 V_{RMS}. The assay begins with a low-voltage measurement phase, where the signal amplitude is set to a constant value of 20 mV_{RMS} and the frequency is varied between 415 Hz and 50 kHz. In the example presented in figure 2, the wounding phase of the assay begins at $t \approx 17.7$ s. During this phase, a cycle of wounding/measurement signals is repeated for a total time of 10 min. In the wounding part of the cycle, which has a duration of approximately one second, the signal amplitude is set to a constant value of 1.2 V_{RMS} and the frequency is set to a constant value of 50 kHz. In the measurement part of the cycle, the generated signal is identical to the measurement signal applied before the wounding phase. Finally, the healing phase of the assay (not shown in figure 2) begins immediately after the wounding phase, and the generated signal in this case is also identical to the initial measurement signal. With this variant of the measurement technique, a set of ten-frequency, low-voltage measurements during the complete wounding phase was obtained for each experiment.

3. Results and discussion

3.1. Impedance analysis of MDCK cells with the alternative measurement scheme

Figure 3 shows the time evolution of the series resistance and capacitance of a microelectrode after seeding it with

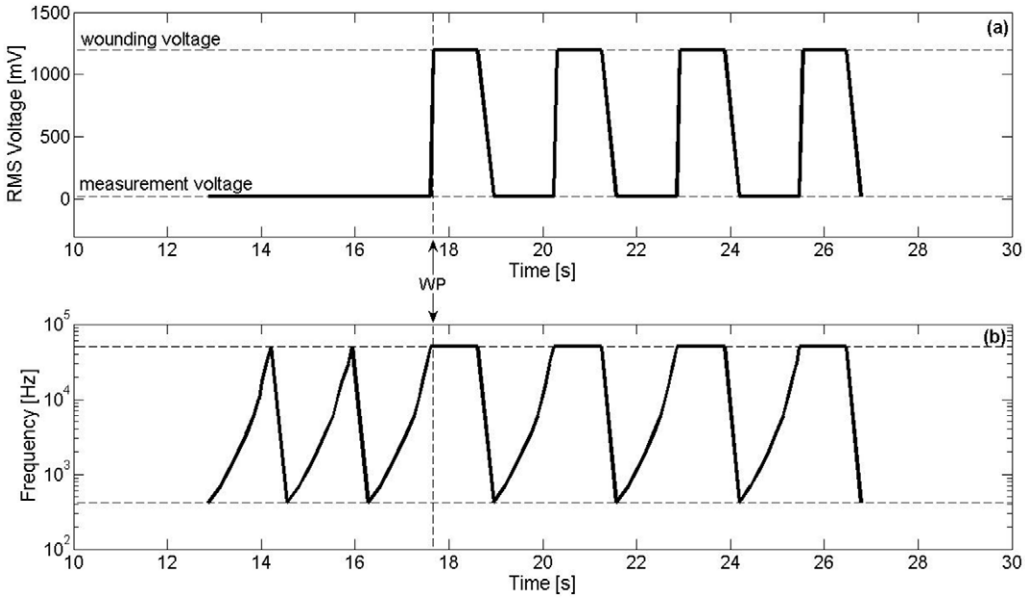

Figure 2. Representation of the wounding signal corresponding to the second measurement strategy employed in this work to register the fast impedance changes during the wounding phase of the assay. The excitation amplitude was in this case 1.2 V_{RMS}. The 'WP' arrows indicate the beginning of the wounding phase. (a) Signal RMS voltage as a function of time. The bottom and top horizontal dashed lines represent the measurement and wounding voltages, respectively. (b) Signal frequency as a function of time. The bottom and top horizontal dashed lines represent the lowest and highest frequencies of the range (415 Hz and 50 kHz, respectively). For clarity purposes, only a portion of the complete signal is shown.

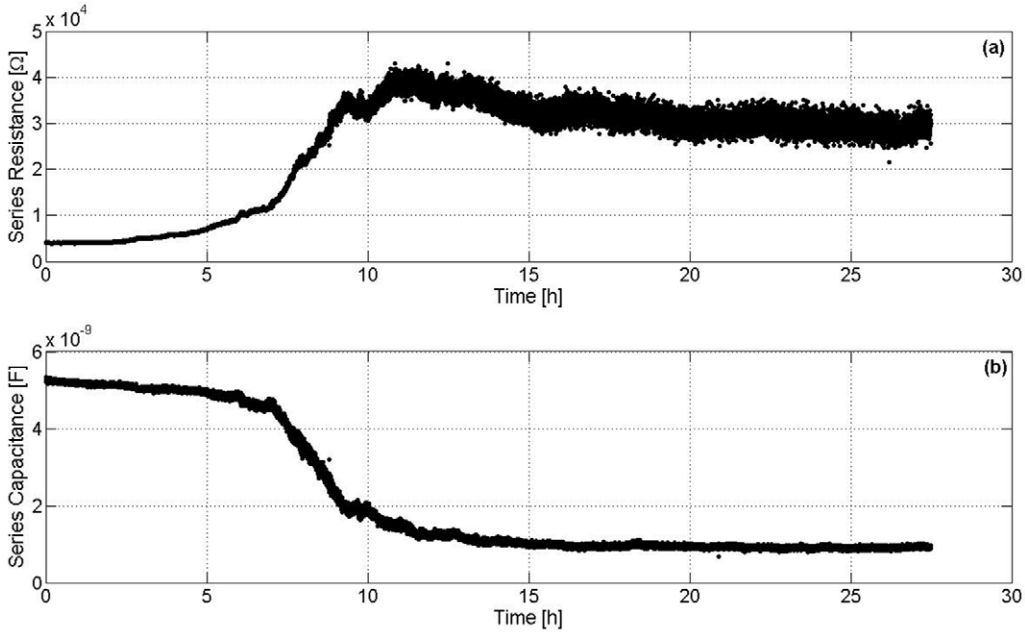

Figure 3. Time evolution of the series resistance and capacitance of a microelectrode after seeding it with MDCK cells, measured with the LCR-meter-based ECIS setup at 20 mV_{RMS} and 3492 Hz. The cells were seeded at $t = 0$. (a) Series resistance as a function of time. (b) Series capacitance as a function of time.

MDCK cells, measured with the LCR-meter at 20 mV_{RMS} and 3492 Hz. It exhibits the typical behaviour of this cell type when cultured under standard conditions, and the results are in concordance with those obtained by means of the traditional measurement scheme [2, 16]. The resistance value increases from approximately 4 kΩ (corresponding to a naked electrode) to approximately 30 kΩ (corresponding to a cell-covered electrode). As it can be observed, after about 20 h the system reaches a stationary state, showing only relatively slight fluctuations which are characteristic of a living cells' culture [21]. Correspondingly, the capacitance value decreases from approximately 5.2 nF to a stationary value of approximately 1 nF. The wounding assays were performed at this stationary stage.

Figures 4(*a*) and (*b*) show the average series resistance and capacitance, respectively, of 10 different microelectrodes

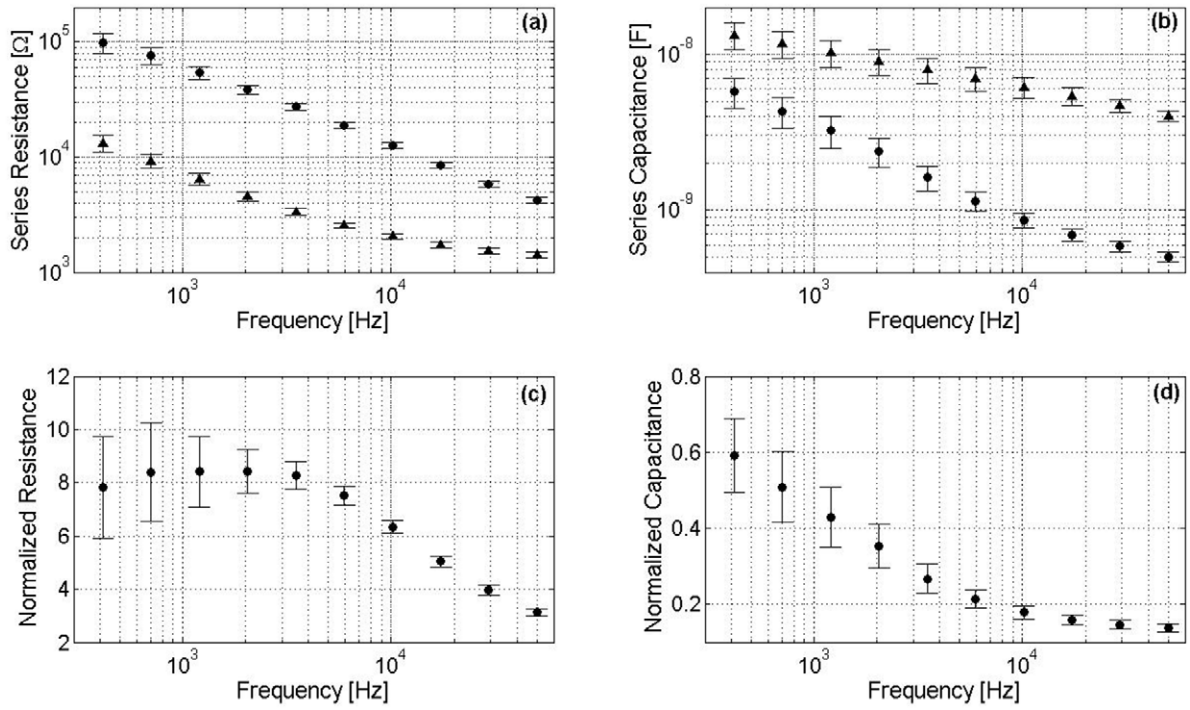

Figure 4. Average electric properties of 10 naked (triangles) and MDCK cell-covered (circles) microelectrodes as a function of frequency, measured with the LCR-meter-based ECIS setup at 20 mV_{RMS} with (a) series resistance, (b) series capacitance, (c) normalized resistance and (d) normalized capacitance. The error bars represent the standard error.

at 10 frequencies between 415 Hz and 50 kHz. Two different data sets are plotted in each figure, one corresponding to the microelectrodes immediately before seeding the cells (i.e. naked microelectrodes) and the other corresponding to the stationary state described before. As it can be appreciated, both the system's resistance and capacitance decrease as the frequency increases, but the form of the curve is modified by the presence of cells. Different models have been presented which describe the alteration of the frequency-dependant impedance of the system when a cell monolayer is attached to the microelectrode [17, 18, 21]. One of these models, originally presented by Giaever and Keese [21], considers the cells as circular discs attached to the electrode surface. The total impedance of the system consists of the measured impedance of the naked electrode, the impedance through the cell layer and the resistivity of the culture medium. Both the basal and apical membranes of the cells are modelled as capacitors in series and two different resistances are associated to the presence of the cells, namely the resistance under the cells and the intercellular resistance. The measured impedance of the cell-covered electrodes is interpreted by modelling the system as an equivalent series *RC* circuit. This model accurately predicts the impedance changes shown in figure 4 for microelectrodes covered with a cell monolayer in the stationary state.

Each curve corresponding to a cell-covered electrode has been normalized by dividing its resistance and capacitance values at each frequency by the corresponding naked electrode's resistance and capacitance, respectively. The results are shown in figures 4(*c*) and (*d*) for the average normalized resistance and capacitance, respectively. The difference between the spectral resistance of naked and cell-covered electrodes is more noticeable in the range of frequencies between 1 and 4 kHz, as indicated by the maximum of the normalized resistance curve. This is a typical behaviour of microelectrodes covered with an MDCK monolayer at the stationary state [18]. The results presented in figure 4 are also in concordance with those obtained previously with the lock-in-based measurement scheme [16]. MDCK cells cause a fall in capacitance and the values differ more with high frequencies, while at low frequencies the curves converge. There the capacitance of the Helmholtz double layer dominates [22]. In all cases, the error in the resistance and capacitance measurements was larger at low frequencies due to a lower precision of the measurement device.

3.2. Electrical response at different voltages

According to previous works, ECIS measurements performed with ac currents in the order of 1 μA_{RMS} have no detectable effects on the cells [2]. A typical electrical wound-healing assay makes use of a high-frequency ac current in the order of 1 mA_{RMS} to induce cell death [2, 23]. In our experiments, the cell-covered electrode's impedance at the highest frequency (50 kHz) has a mean value of approximately 8 kΩ. So, by Ohm's law, to circulate a current of 1 mA_{RMS} it would be necessary to apply a voltage of approximately 8 V_{RMS}, which is beyond the maximum voltage of the employed LCR-meter, namely 2 V_{RMS}. However, we registered a sharp resistance fall (and a corresponding capacitance increase) which is typical of cell wounding assays by applying voltages smaller than 2 V_{RMS}, which correspond to current amplitudes smaller than 0.25 mA_{RMS}.

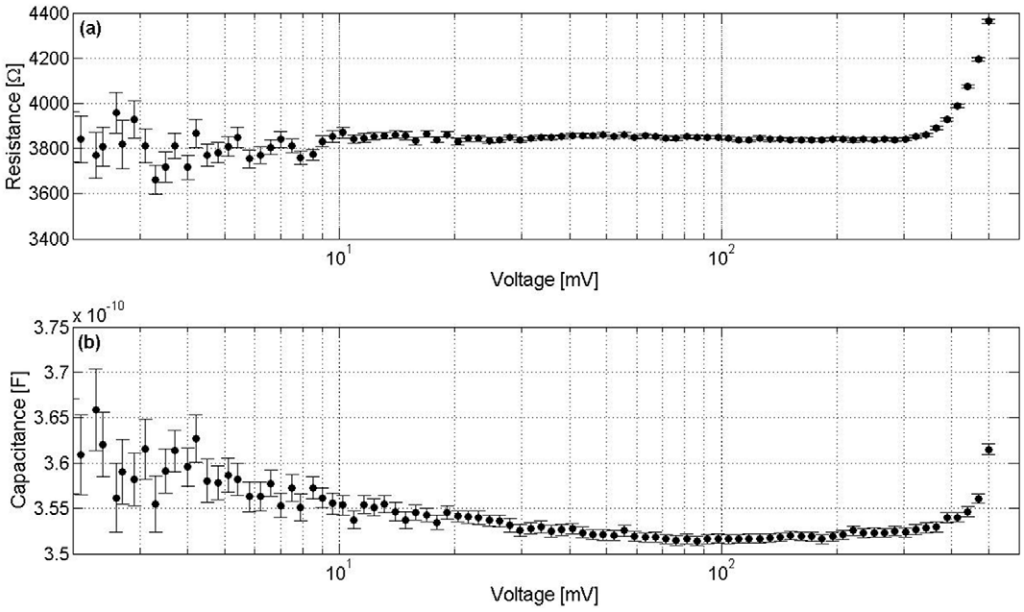

Figure 5. Effect of the signal amplitude on the impedance measurements, performed on a cell-covered electrode at a frequency of 50 kHz with the LCR-meter-based measurement scheme. (a) Series resistance as a function of measurement voltage. (b) Series capacitance as a function of measurement voltage. The error bars represent the standard error.

In order to find the boundary between a non-damaging voltage and a damaging one, a series of measurements were performed in which a voltage sweep was carried out. Figures 5(*a*) and (*b*) show the results corresponding to a low-voltage sweep between 2 and 500 mV_{RMS} at 50 kHz. Every voltage was applied for approximately 1 s with impedance readings at the reference voltage of 20 mV_{RMS} in between. The voltage was increased and decreased 10 times in every experiment. As it can be expected, the noise in the measurement is more noticeable at low voltages; therefore the error bars are larger. At $V \approx 20\,mV_{RMS}$ the error is less than 0.4%, both for the resistance and capacitance, so this amplitude was chosen to carry out non-damaging impedance measurements with low electronic noise.

An interesting behaviour can be observed for voltages higher than approximately 300 mV_{RMS}, where both resistance and capacitance tend to increase over the mean value registered at lower voltages. This phenomenon was observed both in naked and cell-covered electrodes, although it was more noticeable in the latter. These voltage-dependent impedance values indicate that the relation between the applied voltage and the resulting current is non-linear for voltages higher than approximately 300 mV_{RMS}. However, the small error bars for voltages between 300 and 500 mV_{RMS} show that the measurement signal doesn't induce an irreversible alteration on the cells. Impedance spectra were measured before and after the experiment and the results (not shown in the figure) confirm that the voltage sweep did not induce cell wounding.

A different behaviour is observed at voltages higher than 800 mV_{RMS}, as shown in figure 6. In this case, a high-voltage sweep between 400 and 2000 mV_{RMS} was performed at 50 kHz on a cell-covered electrode at the stationary phase. Every voltage was applied for approximately 0.1 s and followed by a 10-frequency measurement at 20 mV_{RMS} (reference). The figure shows only the high-voltage measurements. In this case, as the voltage increases over 800 mV_{RMS}, the resistance decreases and the capacitance increases. After the application of the highest voltage (i.e. 2 V_{RMS}), the return curve describes a trajectory which is under the first curve in the case of resistance (figure 6(*a*) and over it in the case of capacitance (figure 6(*b*)). The impedance changes observed in these hysteresis-like curves indicate that these voltage values induce some damage in the cells. However, the application of a single voltage sweep like the one shown in this figure is not enough to produce an important change in the impedance values due to cell death, because of the short duration of the high-voltage signals in the sweep, which are more likely to induce membrane electroporation [2]. Nevertheless, with a higher exposure time these voltage values are sufficient to induce cell wounding, as will be shown in section 3.3. We based our choice of the wounding voltage range between 1.2 and 2.0 V_{RMS} according to these results.

3.3. Dynamics of cell wounding

A typical time-dependent spectral response of the system, obtained with the lock-in based measurement scheme before and after inducing cell wounding, is shown in figures 7(*a*) and (*b*). The grey zone corresponds to the time interval in which the wounding electrical current was applied. These figures show the two main consequences of the cell wounding, i.e. a sharp fall on the system's resistance and a sharp increase of the system's capacitance. However, as it can be observed, although the measurement was started immediately after the interruption of the wounding signal, it was not possible to plot a time-resolved curve of the resistance drop (or capacitance increase) due to the cell wounding. This indicates that the death of the cells and their consequently separation of the

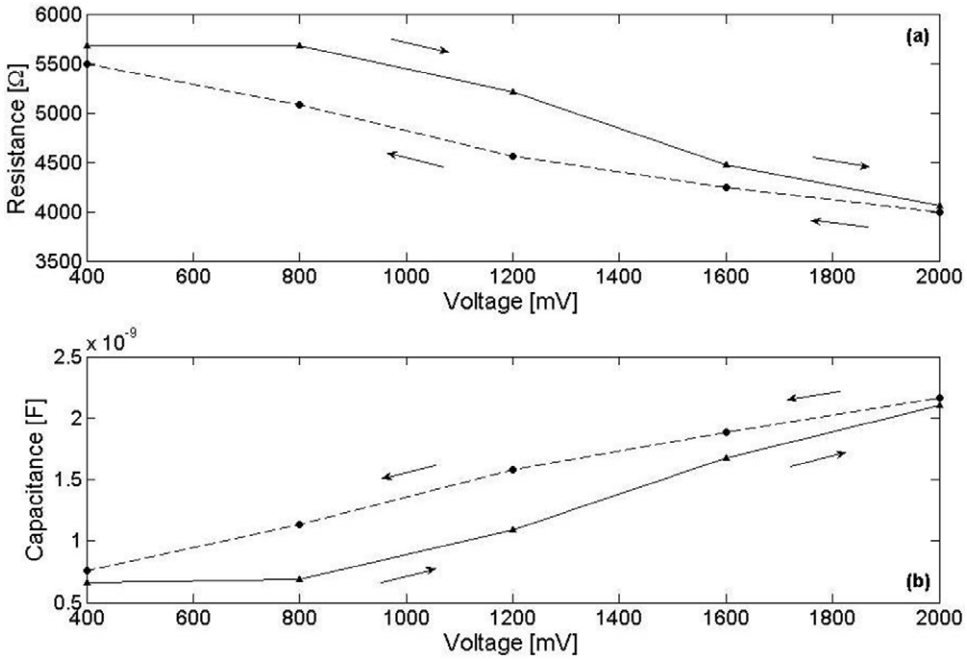

Figure 6. Effect of high measurement voltages on the electrical properties of MDCK cells. The measurements were performed at a frequency of 50 kHz with the LCR-meter-based measurement scheme. The first (ascending) voltage sweep is indicated by the solid lines (triangles), while the dashed lines (circles) represent the second sweep (descending). (a) Series resistance as a function of measurement voltage. (b) Series capacitance as a function of measurement voltage.

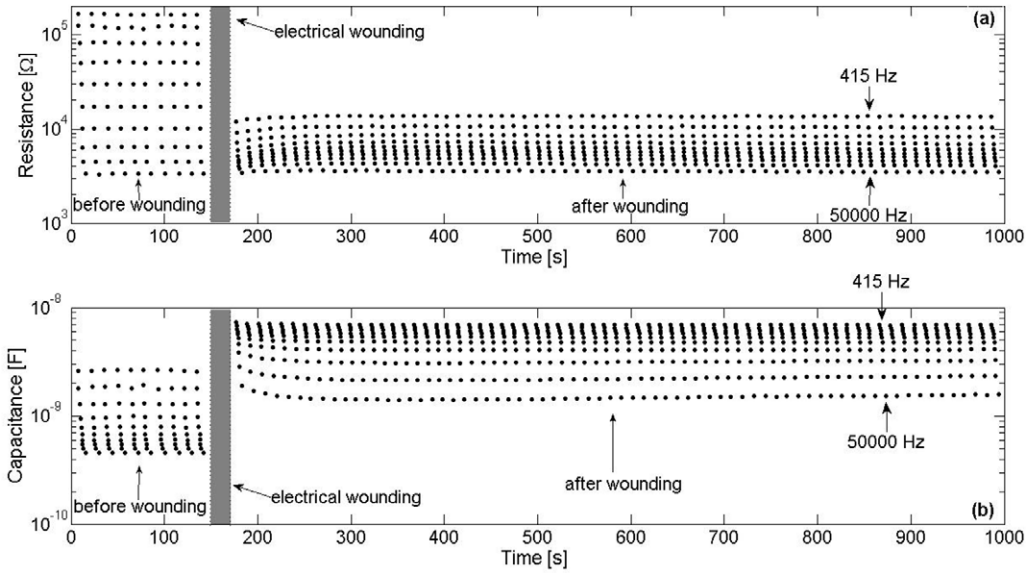

Figure 7. Traditional wound-healing assay, performed with the lock-in-based measurement scheme. (a) Series resistance as a function of time, before and after the wounding process. (b) Series capacitance as a function of time, before and after the wounding process. The higher values in both plots correspond to the lowest measurement frequency, while the lowest values correspond to the highest measurement frequency.

electrode surface take place only while the wounding current is being circulated, after which the system begins to evolve until reaching the original stationary state.

The first attempt to obtain information about the dynamics of the cell wounding was to carry out the wound-healing assay with the alternative measurement scheme, using the wounding signal at $2\,V_{RMS}$ and 50 kHz to take a continuous, single-frequency measurement of the system's impedance. Figure 8(*a*) shows the time evolution of the system's resistance for this experiment, measured before, during and after the wounding process. A nonlinear voltage–current relationship can be observed as a discontinuity in the resistance curve during the application of the wounding signal. We attribute this result to the difference between measurement voltages, namely $20\,mV_{RMS}$ before and after wounding the cells and $2\,V_{RMS}$ during the wounding process. This behaviour was noticed in several similar experiments, and it can also be appreciated in the capacitance curve (figure 8(*b*)).

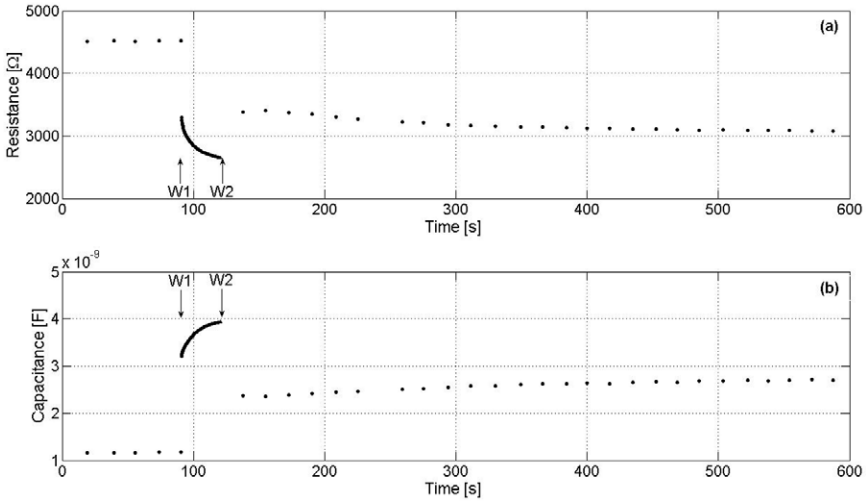

Figure 8. Alternative wound-healing assay, performed with the LCR-meter-based measurement scheme and the first measurement strategy (section 2.3). The wounding signal had an amplitude of $2\,V_{RMS}$ and a frequency of 50 kHz, and it was applied during the time interval indicated between W1 and W2. (a) Series resistance as a function of time, before, during and after the wounding process. (b) Series capacitance as a function of time, before, during and after the wounding process.

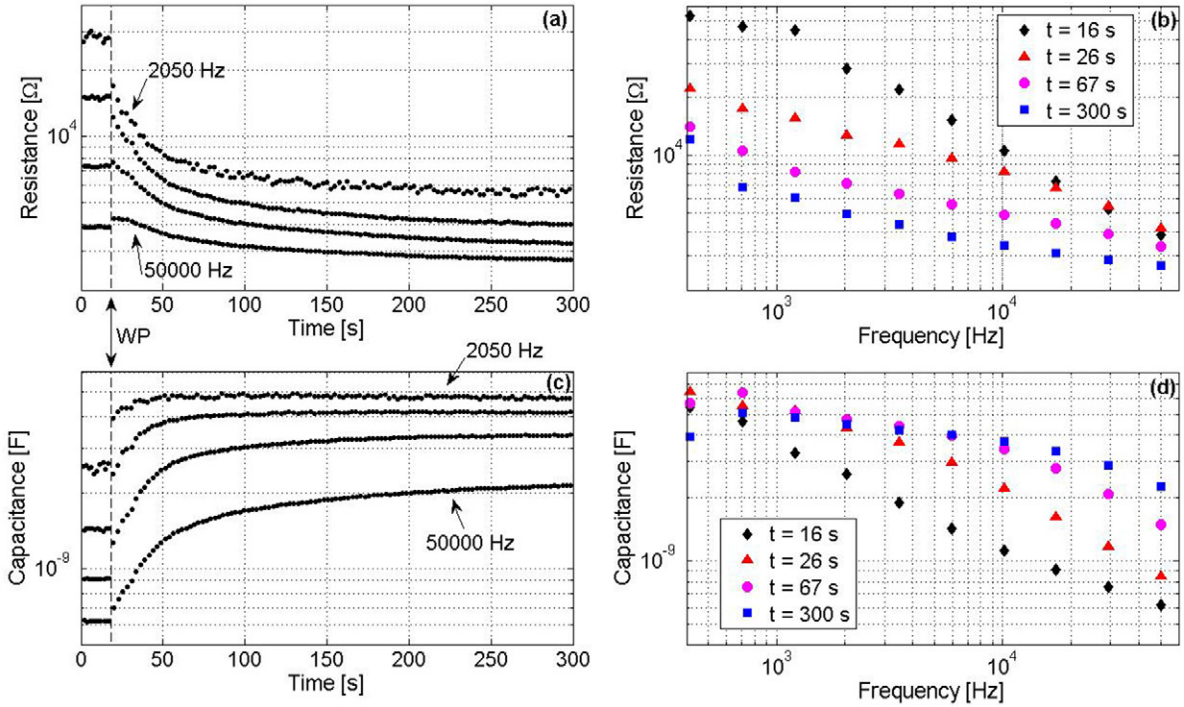

Figure 9. Alternative wound-healing assay, performed with the LCR-meter-based measurement scheme and the second measurement strategy (section 2.3). The dashed lines 'WP' indicate the beginning of the wounding phase. The applied voltage amplitudes were $1.2\,V_{RMS}$ for the wounding signal and $20\,mV_{RMS}$ for the measurement signal. (a) Resistance as a function of time, before, during and after the wounding process. (b) Resistance as a function of frequency at four different time points. (c) Capacitance as a function of time, before, during and after the wounding process. (d) Capacitance as a function of frequency at four different time points. For clarity purposes, only 4 of the 10 measured frequencies were plotted, namely 2.05, 5.95, 17.24 and 50 kHz. The higher values in plots (a) and (c) correspond to the measurements at 2.05 kHz, while the lowest values correspond to a frequency of 50 kHz.

As stated in section 2.3, this measurement strategy presents two main problems, namely the discontinuity in the resistance and capacitance curves and the fixed measurement frequency. To solve the previous issues, an experiment was conducted employing the second measurement strategy (section 2.3) and the results are shown in figure 9. At the beginning of the wounding phase, the measurement voltage of $20\,mV_{RMS}$ was switched to the wounding voltage of $1.2\,V_{RMS}$. The wounding current was circulated for 1 s, after which the voltage was switched again to $20\,mV_{RMS}$ and a 10-frequency measurement was taken. This procedure was repeated until the system was exposed to the $1.2\,V_{RMS}$ signal for a total time of 10 min. The mean duration of the low-voltage measurements was 1.2 s, and the amplitude of the wounding current varied

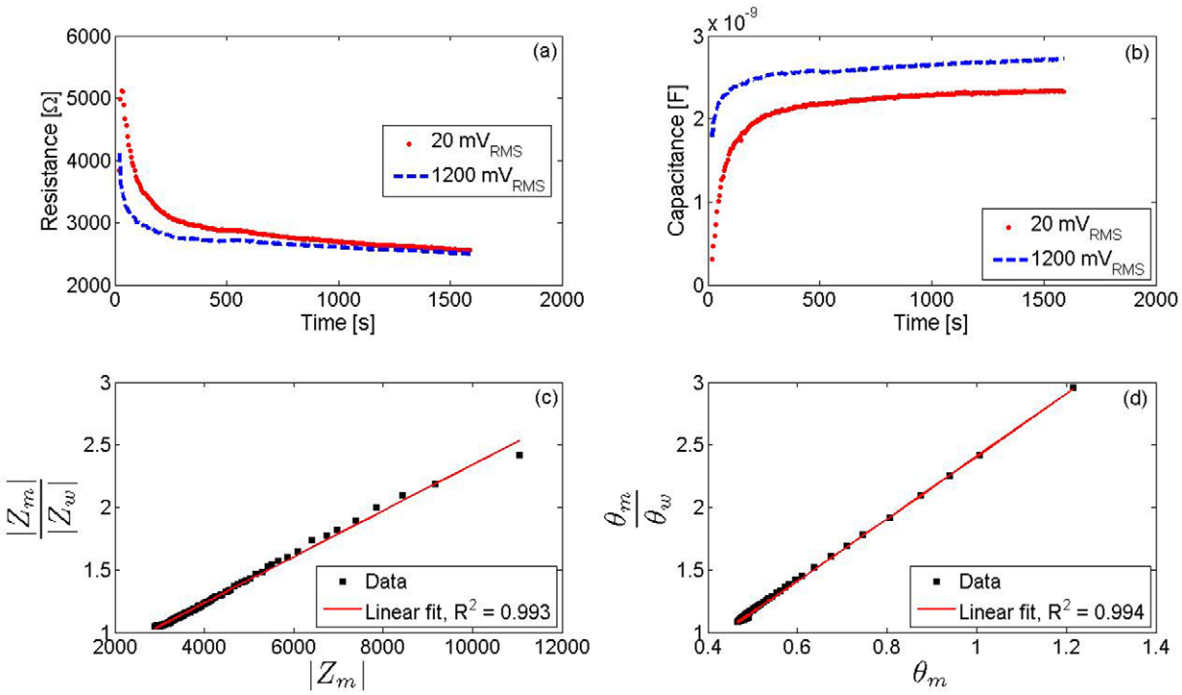

Figure 10. Empirical correlation between high- and low-voltage measurements during an alternative wound-healing assay employing the second measurement strategy (section 2.3). (a) Resistance and (b) capacitance as a function of time. The red circles represent the values measured at 20 mV_{RMS} and the dashed blue lines represent the values measured at 1.2 V_{RMS}. (c) Ratio of impedance magnitudes as a function of the low-voltage impedance magnitude. (d) Ratio of phase angles as a function of the low-voltage phase angle.

between 0.2 and 0.3 mA_{RMS}. Figures 9(*b*) and (*d*) show the resistance and capacitance spectra, respectively, at 4 different time points during the experiment. At $t = 16$ s, the spectra correspond to the cell-covered electrode immediately before the wounding phase. As time increases, the wound progresses and both the resistance and capacitance curves move towards the corresponding naked electrode's curves (see figures 4(*a*) and (*b*)), reaching a stationary state after applying the wounding signal for approximately 5–10 min. As it can be observed, this experiment made it possible to plot a time-resolved spectral response of the system's resistance and capacitance during the wounding process. In contrast with the previous measurement strategy (figure 8), here the measurement voltage was the same before and during the wounding, namely 20 mV_{RMS}. The impedance values measured with the wounding signal were also registered, although they are not shown in figure 9.

3.4. Correlation between low- and high-voltage measurements

The resistance and capacitance curves obtained with the wounding signal in the previous experiment showed the same nonlinear behaviour as in figure 8. However, in this case a comparison between high- and low-voltage measurements can be done. In fact, during the wounding phase there are several low- and high-voltage measurement cycles. The time between the last measurement at low voltage and the first measurement at high voltage in a round is about 0.1 s, and the frequency of both measurements is the same, namely 50 kHz (figure 2). So, if we assume that the system is only slightly altered in this time interval, we can compare the impedance values at high and low voltage during the wounding phase, at a frequency of 50 kHz, to obtain an empirical correlation. A typical result is shown in figure 10 for a wounding voltage of 1.2 V_{RMS}. The resistive and capacitive parts of the impedance at both excitation amplitudes are plotted as a function of time in figures 10(*a*) and (*b*), respectively.

Figure 10(*c*) shows that the ratio of the impedance magnitude at low and high voltages is proportional to the impedance magnitude at low voltage, and the same correlation was found for the phase angles (figure 10(*d*)). This empirical correlation can be expressed as

$$\frac{|Z_m|}{|Z_w|} = a_1.|Z_m| + b_1 \tag{1}$$

$$\frac{\theta_m}{\theta_w} = a_2.\theta_m + b_2 \tag{2}$$

In these equations, $|Z_m|$ and θ_m represent the low-voltage impedance magnitude and phase angle, respectively, while $|Z_w|$ and θ_w represent the high-voltage impedance magnitude and phase angle, respectively. These quantities are computed from the resistance and capacitance readings by applying the following equations, corresponding to a series *RC* circuit:

$$|Z| = \sqrt{R^2 + \left(\frac{1}{2.\pi.f.C}\right)^2} \tag{3}$$

$$\theta = \tan^{-1}\left(\frac{1}{2.\pi.f.C.R}\right) \tag{4}$$

Table 1. Correlation parameters at the extreme voltages of the wounding interval.

Voltage amplitude [V_{RMS}]	$a_1 \times 10^4$ (Ω^{-1})	b_1	a_2 (rad^{-1})	b_2
1.2	1.8 ± 0.6	0.49 ± 0.11	2.0 ± 0.4	0.1 ± 0.2
2.0	3.0 ± 0.4	0.28 ± 0.10	2.86 ± 0.18	− 0.12 ± 0.11

where R and C are the measured series resistance and capacitance, respectively, and f is the measurement frequency. Note that, instead of using the actual phase angles of the equivalent series RC circuits (which are always negative), we used their absolute values in equations (2) and (4). This was done deliberately in order to obtain a line with positive slope in figure 10(*d*), which is easier to interpret.

This fitting was performed at 1.2 V_{RMS} on 18 wounding curves obtained from different electrodes of the same size and geometry, all of which showed a similar behaviour. However, this effect was observed only in cell-covered electrodes, whereas the impedance values of the naked electrodes at high and low voltages were not correlated. We want to stress here that this particular correlation is empirical and not necessarily holds for other electrode sizes and cell types. In order to compare the correlation parameters at both extremes of the wounding interval, the experiment was also conducted at 2 V_{RMS} on 10 different cell-covered electrodes. The results are presented in table 1.

The results show that the higher the voltage amplitude the higher the parameters a_1 and a_2, which indicates that the nonlinearity increases with the excitation amplitude.

4. Conclusions

A fast impedance measurement setup was employed to determine the spectral resistance and capacitance of naked and cell-covered microelectrodes and the results are in concordance with those obtained at lower speed with the traditional ECIS measurement scheme. For MDCK cells, we found that nonlinear effects appear in the impedance measurements at voltages higher than 300 mV_{RMS}. Additionally, the boundary between non-damaging and damaging signals for this cell line with this measurement scheme was found at approximately 800 mV_{RMS} (current amplitude of approximately 0.1 mA_{RMS}).

A measurement technique was introduced which is capable of monitoring the temporal variation of the spectral resistance and capacitance for cell-covered electrodes during the fast wounding phase of a wound-healing assay. With this data it is possible to plot time-resolved curves of the resistance fall and capacitance increase during cell wounding. The characteristic duration of this transient regime was found to be in the order of 10 min for MDCK cells with a wounding signal of 1.2 V_{RMS} and 50 kHz, applied as a series of cycles consisting of 1 s of a high-voltage signal followed by 1 s of a low-voltage measurement. This procedure is different to those previously established, where the wounding current was applied continuously and complete cell killing was observed at shorter times.

An empirical correlation was found between impedance measurements at high and low voltages during the wounding phase of the assay and the correlation parameters were determined for two different wounding voltages. The nonlinearity of the voltage–current relationship was found to increase with the excitation amplitude.

Different electrode sizes and cell types should be tested in order to analyse the dependence of the correlation parameters with these variables. Moreover, a deeper analysis of the nonlinearities present in impedance measurements of cell-covered electrodes should be carried out, for which the measurement technique introduced in this work would prove helpful. Electrode polarization effects were not considered in this paper but should also be analysed as a potential source of nonlinearities. Microscopic observations should also be taken into account, for which the opaque multiwell used in this work must be replaced with a transparent one. Finally, as an alternative setup the measurement device could be modified to produce a multi-frequency wounding signal. Both the wounding capability of this alternative method and the resulting impedance measurements should then be evaluated in order to determine whether it can be used to obtain relevant information during the wounding phase of the assay.

Acknowledgments

We thank Applied BioPhysics Inc. for providing the ECIS Cultureware™ multiwell. F E G acknowledges a scholarship from CONICET, Argentina.

References

[1] Riahi R, Yang Y, Zhang D and Wong P 2012 Advances in wound-healing assays for probing collective cell migration *J. Lab. Autom.* **17** 59–65

[2] Keese C, Wegener J, Walker S and Giaever I 2004 Electrical wound-healing assay for cells *in vitro Proc. Natl Acad. Sci.* **101** 1554–9

[3] Giaever I and Keese C 1984 Monitoring fibroblast behaviour in tissue culture with an applied electric field *Proc. Natl Acad. Sci. USA* **81** 3761–4

[4] Giaever I and Keese C 1986 Use of electric fields to monitor the dynamical aspect of cell behaviour in tissue culture *IEE Trans. Biomed. Eng.* **BME-33** 242–7

[5] Bagnaninchi P and Drummond N 2011 Real-time label-free monitoring of adipose-derived stem cell differentiation with electric cell-substrate impedance sensing *Proc. Natl Acad. Sci.* **108** 6462–7

[6] Mueller J, Thirion C and Pffafl M 2011 Electric cell-substrate impedance sensing (ECIS) based real-time measurement of titer dependent cytotoxicity induced by adenoviral vectors in an IPI-2I cell culture model *Biosensors Bioelectron.* **26** 2000–5

[7] Åberg P, Nicander I, Hansson J, Geladi P, Holmgren U and Ollmar S 2004 Skin cancer identification using multifrequency electrical impedance—a potential screening tool *IEEE Trans. Biomed. Eng.* **51** 2097–102

[8] Das D, Kamil F, Biswas K and Das S 2012 Electrical characterization of suspended HeLa cells using ECIS based biosensor *6th Int. Conf. on Sensing Technology (ICST) IEEE* pp 734–7
[9] Bellotti M, Bast W, Berra A and Bonetto F 2011 A new experimental device to evaluate eye ulcers using a multispecral electrical impedance technique *Rev. Sci. Instrum.* **82** 074303
[10] Yarrow J, Perlman Z, Westwood N and Mitchison T 2004 A high-throughput cell migration assay using scratch wound healing, a comparison of image-based readout methods *BMC Biotechnol.* **4** 21
[11] Rodriguez L, Wu X and Guan J 2005 Wound-healing assay *Methods Mol. Biol.* **294** 23–9
[12] Környei Z, Czirók A, Vicsek T and Madarász E 2000 Proliferative and migratory responses of astrocytes to *in vitro* injury *J. Neurosci. Res.* **61** 421–9
[13] Mondal N, Mondal D and RoyChaudhuri C 2011 A simple and sensitive cytosensor based electrical characterization of *in vitro* wound healing assay for keratinocytes *IEEE/NIH Life Science Systems and Applications Workshop (LiSSA)* pp 47–50
[14] Linderholm P, Braschler T, Vannod J, Barrandon Y, Brouard M and Renaud P 2006 2D impedance imaging of cell migration and epithelial stratification *Lab Chip* **6** 1155–62
[15] Richardson J, Scalera V and Simmons N 1981 Identification of two strains of MDCK cells which resemble separate nephron tubule segments *Biochim. Biophys. Acta* **673** 26–36
[16] Wegener J, Keese C and Giaever I 2000 Electric cell-substrate impedance sensing (ECIS) as a noninvasive means to monitor the kinetics of cell spreading to artificial surfaces *Exp. Cell Res.* **259** 158–66
[17] Wegener J, Sieber M and Galla H 1996 Impedance analysis of epithelial and endothelial cell monolayers cultured on gold surfaces *J. Biochem. Biophys. Methods* **32** 151–70
[18] Lo C, Keese C and Giaever I 1995 Impedance analysis of MDCK cells measured by electric cell-substrate impedance sensing *Biophys. J.* **69** 2800–7
[19] Freshney R 1994 *Culture of Animal Cells* 3rd edn (New York: Wiley) pp 149–59
[20] *Agilent Impedance Measurement Handbook* 2009 4th edn (Santa Clara CA: Agilent Technologies) pp 3–4
[21] Giaever I and Keese C 1991 Micromotion of mammal cells measured electrically *Proc. Natl Acad. Sci. USA* **88** 7896–900
[22] Borkholder D 1998 Cell-based biosensors using microelectrodes *PhD Thesis* Stanford University (http://www.researchgate.net/profile/David_Borkholder/publication/245625743_Cell_Based_Biosensors_using_Microelectrodes/links/5421e7f10cf2a39f7671b.pdf?origin=publication_detail)
[23] Keese C and Giaever I 2013 Automated cell migration assay (www.biophysics.com/woundhealingpubs.php)